*Int. J. Heat Mass Transfer.* Vol. 32, No. 5, pp. 825–835, 1989
Printed in Great Britain

0017–9310/89 $3.00 + 0.00


# Boundary layer nucleation

S. S. CHA
Department of Mechanical Engineering, University of Illinois at Chicago,
P.O. Box 4348, Chicago, IL 60680, U.S.A.

and

R. K. AHLUWALIA and K. H. IM
Engineering Division, Argonne National Laboratory, 9700 South Cass Avenue,
Argonne, IL 60439, U.S.A.

(*Received* 24 *November* 1987 *and in final form* 9 *September* 1988)

**Abstract**—Nucleation and transport of a condensable trace species across subcooled laminar/turbulent boundary layers are investigated. Spontaneous homogeneous nucleation is found to occur for surfaces maintained at temperatures much below the dew point. The embryos so formed provide condensation sites for heterogeneous nucleation. The effect of boundary layer condensation is always to diminish the mass transfer of trace species. There is an intermediate temperature range where the decrease in vapor deposition is not fully compensated by the ensuing Brownian/thermophoretic deposition of particulates so that the combined particle and vapor mass transfer decreases with surface subcooling. For laminar flow, a vapor-free zone is created adjacent to the subcooled surface by direct vapor condensation on the entrained particulate matter. The mass transfer then occurs solely due to particulate deposition mechanisms. For turbulent flow, vapor mass transfer persists even at low surface temperatures. A significant decrease in net deposition flux is observed partly due to turbulent back diffusion of particles into the superheated zone and, more importantly, due to strong turbulent convection.

## 1. INTRODUCTION

IN SOME applications, the problem of mass transfer of a trace species from a superheated stream to a subcooled surface is encountered [1, 2]. A recent study [1] identified three critical surface temperatures that are important in the mass transfer process. These correspond respectively to the dew point, localized boundary layer supersaturation, and commencement of homogeneous nucleation in the supersaturated boundary layer. Two major simplifications are invoked in the study.

(1) Explicit convection terms are dropped from the conservation equations.
(2) The growth of the nucleated particles due to direct vapor condensation (heterogeneous nucleation) is neglected.

The objectives of this work are to relax these two assumptions and to confirm the existence of an intermediate surface temperature range where mass transfer decreases with surface subcooling. The principal motivation lies in our knowledge that, under most conditions of temperature, pressure, and concentration, gas phase condensation occurs primarily through vapor condensation on the sites provided by the homogeneous nucleation process, and that gas phase mass transfer committed to the formation of embryos is negligible [3, 4].

## 2. THEORY

As in ref. [1], we consider the convective flow of a stream, containing a trace amount of condensable impurity vapor, over a subcooled surface. The free stream is superheated with respect to the vapor the concentration of which is sufficiently dilute ($Y < 10^{-5}$) to render negligible the effects of condensation on heat transfer and fluid mechanics. The unperturbed flow and temperature fields are determined from numerical solution of the classical boundary layer equations [5]. For turbulent boundary layers, a mixing length hypothesis is employed to compute the eddy viscosity [6]

$$\mu_t = \rho l^2 \left|\frac{\partial u}{\partial y}\right|. \tag{1}$$

In the inner turbulent region of the boundary layer

$$l = 0.435y[1 - \exp(-y/A)] \tag{2}$$

with

$$A = 26\nu(\tau/\rho)^{-1/2}. \tag{3}$$

In the outer region

$$l = 0.09\delta. \tag{4}$$

The turbulent Prandtl number for calculation of thermal diffusivity is taken as

## NOMENCLATURE

| | |
|---|---|
| $C_m$ | momentum jump coefficient (3.32) |
| $C_t$ | temperature jump coefficient (1.0) |
| $D$ | diffusivity |
| $J$ | nucleation rate |
| $k$ | thermal conductivity |
| $Kn$ | Knudson number |
| $l$ | mixing length |
| $MW$ | molecular weight |
| $n$ | distribution function |
| $P$ | pressure |
| $Pr$ | Prandtl number |
| $r$ | particle radius |
| $r^*$ | critical radius |
| $\dot{r}$ | growth rate |
| $R$ | gas constant |
| $Re_x$ | Reynolds number based on distance |
| $S$ | supersaturation |
| $St_m$ | Stanton number for mass transfer |
| $T$ | temperature |
| $u$ | axial velocity |
| $v$ | transverse velocity |
| $v_{th}$ | thermophoretic velocity |
| $W$ | deposition flux |
| $x$ | axial coordinate |
| $y$ | normal coordinate |
| $Y$ | mass fraction. |

Greek symbols

| | |
|---|---|
| $\alpha$ | ratio of particle to gas thermal conductivity |
| $\delta$ | boundary layer thickness |
| $\mu$ | viscosity |
| $\nu$ | kinematic viscosity |
| $\rho$ | density |
| $\sigma$ | surface tension |
| $\tau$ | shear stress. |

Subscripts

| | |
|---|---|
| d | dew point |
| l | liquid |
| p | particle |
| s | saturation |
| t | turbulent |
| v | vapor |
| w | wall |
| $\infty$ | free stream. |

$$Pr_t = 0.9\left[\frac{1-\exp(-y/A)}{1-\exp(-y/B)}\right] \quad (5)$$

where

$$B = \frac{35}{26}A. \quad (6)$$

### 2.1. *Particle field*

In a subcooled boundary layer, the supersaturation ratio may exceed the critical value for onset of homogeneous nucleation in a dust-free gas. This results in the formation of angstrom-sized embryos which are subject to fluid convection, Brownian diffusion normal to the flow direction, transport by turbulent eddies, and thermophoretic diffusion due to temperature gradients in the thermal boundary layer. The embryos also provide sites for direct condensation of vapor and consequently grow in size. A particle size spectrum develops because of the aging distribution with respect to particle formation. The evolution of the size distribution is described by the following population balance equation:

$$\frac{\partial}{\partial x}(un) + \frac{\partial}{\partial y}[(v+v_{th})n] + \frac{\partial}{\partial r}(\dot{r}n) = \frac{\partial}{\partial y}\left(D_p\frac{\partial n}{\partial y}\right) + J(r)\delta(r-r^*). \quad (7)$$

The following boundary conditions, appropriate for a superheated stream and a perfectly absorbing wall, are imposed on $n$:

$$n(x, \infty, r) = 0 \quad (8)$$

$$n(x, 0, r) = 0. \quad (9)$$

Equation (7) describes the formation, growth, diffusion, and forced convection of particles. It is different from the treatment in ref. [1] because of the inclusion of the forced convection and growth terms. The common features are summarized below.

(a) The classical nucleation theory is employed to calculate the homogeneous nucleation rate ($J$). The critical size of the embryos is determined from the Gibbs–Thomson relationship. The effect of turbulent fluctuations in gas temperature on embryo stability has been neglected. This is potentially an important phenomenon which deserves further attention. In general, since the embryo vaporization time is smaller than the relevant turbulence time scale, the critical supersaturation ratio for onset of nucleation should be higher than estimated from the classical nucleation theory.

(b) The effective diffusivity of the particles is taken as the sum of the Brownian and turbulent diffusivities. The Brownian diffusivity is estimated from the Stokes–Einstein relationship modified for the Cunningham correction factor. A constraint is imposed that the Brownian diffusivity should not exceed the kinematic diffusivity, estimated from the kinetic theory of gases, of the embryo regarded as a macro molecule. For the particle size of interest (particle response frequency is much greater than the frequency of energy-containing turbulent eddies), the particles

are assumed to follow the turbulent fluctuations and have turbulent diffusivity identical with the eddy viscosity estimated from the mixing length theory [7].

(c) A particle suspended in a gas with an imposed temperature gradient experiences a thermal force producing motion directed toward lower temperatures. The magnitude of the thermophoretic velocity depends strongly upon the Knudson number of the particle and is directly proportional to the temperature gradient. After Springer [8], we adopt the following representation for $v_{th}$:

$$v_{th} = \frac{v_{th}^*}{1+f(Kn)} \tag{10}$$

where $v_{th}^*$ is the well-accepted formula in the free-molecular limit ($Kn \gg 1$)

$$v_{th}^* = -\left(\frac{8Cn}{45}\right)\frac{(kr/\mu)}{(2\pi RT)^{1/2}}\frac{\partial T}{\partial y} \tag{11}$$

and $f$ is an interpolation formula between free molecular and continuum regimes

$$f(Kn) = \left(\frac{2}{9Kn}\right) \times \frac{1+2\alpha+Kn[2C_t+3C_m(1+2\alpha+2C_t\,Kn)]}{\alpha+Kn[C_t+3.2C_m(\alpha+C_t\,Kn-1)]}. \tag{12}$$

Because of the neglect of the growth rate, ref. [1] used the free molecular limit of $v_{th}$ (i.e. $v_{th}^*$).

### 2.2. *Growth rate*

After Fuchs [9], we adopt a simple formula for interpolating the growth rate between the well-known free-molecular and diffusion limit expressions

$$\dot{r} = F(Kn_v)\left(\frac{\rho_s}{\rho_l}\right)\left(\frac{D_v}{r}\right)\left[S-\exp\left(\frac{\phi}{R_vT}\right)\right] \tag{13}$$

with

$$F(Kn_v) = \frac{1+Kn_v}{1+7.104Kn_v+\frac{4}{3}Kn_v^2}. \tag{14}$$

In the foregoing formula, $\phi$ is two-thirds of the surface tension energy of the droplet per unit mass. It enters the expression through Kelvin's correction to the saturation pressure for surface curvature of a small droplet. It is particularly important for embryo-sized particles. Consistent with the Gibbs–Thomson relationship, vapor condensation is not initiated until $S$ becomes greater than $\exp(\phi/R_vT)$, i.e. a slight subcooling is required.

### 2.3. *Vapor field*

The vapor conservation equation of ref. [1] is modified by inclusion of the convection and growth rate terms

$$\rho u\frac{\partial Y}{\partial x}+\rho v\frac{\partial Y}{\partial y} = \frac{\partial}{\partial y}\left(\rho D_v\frac{\partial Y}{\partial y}\right)-\frac{4}{3}\pi r^{*3}\rho_l J - \int_0^\infty 4\pi\rho_l r^2\dot{r}n\,dr. \tag{15}$$

The boundary conditions are specified free-stream mass fraction (less than the saturation value at $T_\infty$) and $Y_w$ corresponding to the saturation pressure at the wall temperature

$$Y(x,\infty) = Y_\infty \tag{16}$$

$$Y(x,0) = \frac{P_s(T_w)}{P}\left(\frac{MW_v}{MW}\right). \tag{17}$$

As for particle diffusivity, $D_v$ is composed of laminar and turbulent contributions. The former is estimated from the kinetic theory of gases and the latter is equated to eddy viscosity.

## 3. NUMERICAL SOLUTION

The mass transfer equations are solved in a manner analogous to the hydrodynamic equations. Some of the salient features of the solution technique are summarized below.

(a) The conservation equations are transformed into von Mises coordinates. The transformation enables the elimination of the transverse velocity $v$ from the equations. For convenience, the distribution function $n$ is also transformed to a spectral mass fraction quantity defined as

$$\hat{Y}_p(x,y,r) = \frac{4}{3}\pi r^3\left(\frac{\rho_l}{\rho}\right)n. \tag{18}$$

(b) The thermophoretic convection term is discretized by using the upwind differencing scheme. For a cooled surface, the transverse component $v_{th}$ is always directed toward the surface. The appearance of the transverse convection term in the transformed coordinates is peculiar to the particle transport equation.

(c) The particle size grid is resolved by using 24 size bins. The growth term transports the particles between the adjoining size bins. The task of simultaneously solving the size bin equation was avoided by assuming instant vaporization of particles diffused into superheated zones and by using upwind differencing for the growth term. This allows the inversion of the tri-diagonal equations sequentially starting from the smallest size node.

(d) The delta function multiplying the nucleation rate term in the particle conservation equation is approximated as the inverse of the size of the grid bounding $r^*$.

(e) The vapor conservation equation is strongly linked to the population balance equation through the source terms for homogeneous nucleation and heterogeneous nucleation. We prefer solving the cor-

Table 1. Parameter range

| |
|---|
| Medium = air Trace species = $Na_2SO_4$ $\rho_l = 2680\ kg\ m^{-3}$ |
| $\sigma_l = 0.2\ N\ m^{-1}$ $T_\infty = 1350\ K$ $T_w = 400$–$1300\ K$ |
| $u_\infty = 5\ m\ s^{-1}$ (laminar), $10\ m\ s^{-1}$ (turbulent) |
| $Y_\infty = 1$ p.p.m. |
| $\ln P_s(atm) = 7.884 - 2.223 \times 10^4/T - 7.555 \times 10^6/T^2$ |

responding finite-difference equations sequentially rather than iteratively. This restricts us to a small axial step size. An internal numerical estimate on vapor species mass balance is maintained by utilizing the computed particle size spectrum, vapor mass fraction profile, particle deposition, and vapor deposition. The step size is chosen such that the combined particle and vapor mass imbalance defined as

(out convection + deposition − in convection)/

(in convection)

does not exceed a prescribed tolerance (typically $10^{-6}$).

## 4. RESULTS AND DISCUSSION

Illustrative calculations have been performed for deposition of trace $Na_2SO_4$ vapor on a subcooled surface. Table 1 summarizes the range of variables used in the calculations. Air is assumed to be the gaseous medium the density of which is approximated by the equation of state for ideal gases, viscosity by Sutherland's equation, and thermal conductivity as directly proportional to the gas temperature. The molecular diffusivity and mean-free path of $Na_2SO_4$ are estimated from the kinetic theory of gases. For simplicity, in the case of turbulent flow, the transition is presumed to occur from the leading edge of the subcooled surface.

### 4.1. *Laminar flow*

Figure 1 depicts the influence of surface subcooling and flow Reynolds number on $Na_2SO_4$ deposition flux. As in ref. [1], deposition is initiated once the surface is cooled below the dew point. The deposition flux increases precipitously with surface subcooling until a critical surface temperature is reached corresponding to which a portion of the boundary layer attains the supersaturation required for onset of homogeneous nucleation. Below the critical surface temperature, vapor-to-particle conversion causes a steep decline in vapor mass transfer which is compensated in part by the ensuing Brownian and thermophoretic deposition of the particles formed from gas phase condensation. There is an intermediate surface temperature regime where the combined particle and vapor deposition decreases with surface subcooling. Also, except at very low surface temperatures, the combined deposition is smaller than vapor deposition calculated by ignoring the nucleation process.

As the Reynolds number increases, the surface temperature associated with null vapor deposition flux shifts towards the dew point (Fig. 1(b)). This is primarily because of greater entrained particulate loading and boundary layer thickness augmenting gas phase condensation. The combined particle and vapor mass transfer approaches that calculated from ignoring the nucleation processes although the deposition mode is different, i.e. particle vs vapor transport.

Effects of particle convection and heterogeneous nucleation on mass transfer may be ascertained from a qualitative comparison with results presented in ref. [1]. Inclusion of direct condensation on embryos leads to a faster depletion of vapor and eventual vanishing of vapor mass transfer. In ref. [1], the vapor deposition mode was observed to persist even at low surface temperatures. For laminar flow, the combined particle and vapor mass transfer was found to exceed the $Na_2SO_4$ deposition flux calculated from ignoring the possibility of the gas phase nucleation processes. Neglect of convection in ref. [1] amounts to assuming that the nucleation rate integrated over the boundary layer thickness equals the particulate deposition flux. With convection included, Fig. 2 shows the fraction of particles deposited to that formed from homogeneous and heterogeneous nucleation in the boundary layer. The two quantities are defined by the following equations:

$$\text{Particle deposition flux} = \int_0^\infty \frac{4}{3}\pi r^3 \rho_l v_w n\, dr \quad (19)$$

Local condensation rate

$$= \int_0^\infty \frac{4}{3}\pi r^{*3} \rho_l J\, dy + \int_0^\infty dy \int_0^\infty 4\pi r^2 \dot{r} \rho_l n\, dr. \quad (20)$$

Figure 3 exhibits the influence of gas phase condensation on the vapor concentration profile. Consistent with the vapor mass transfer behavior observed in Fig. 1, the concentration gradient at the surface decreases with subcooling. A region close to the surface can be identified which is nearly void of the condensable vapor. The void region, which was not observed in ref. [1], is a manifestation of vapor condensation on the entrained particulates. The width of the void region increases with flow Reynolds number and entrained particulate loading.

Figure 4 displays the variation of aerosol density across the particle boundary layer identified with the location where the gas temperature equals the dew point of the impurity vapor (see Fig. 5 for $\delta_p/\delta$ as a function of wall temperature). The aerosols are formed within the boundary layer. Thermophoresis acts to confine the particles close to the cooled surface whereas Brownian motion causes dispersion. In the region between the surface and peak in aerosol

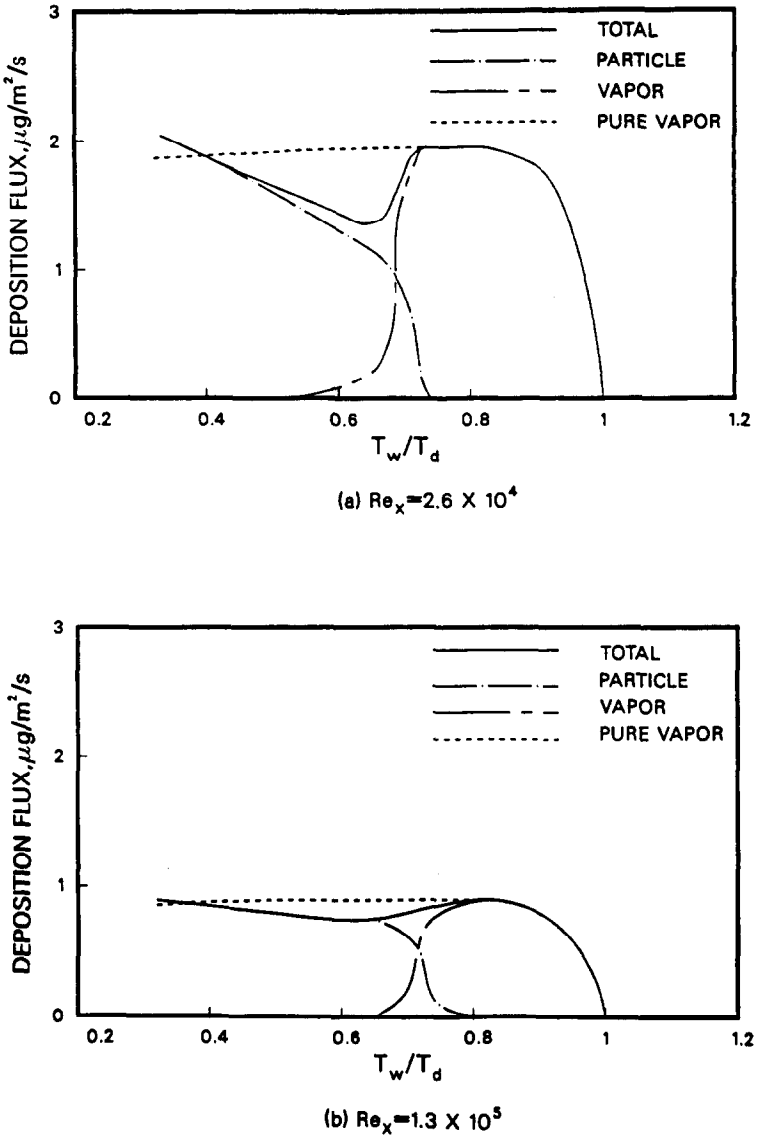


FIG. 1. Particle and vapor deposition in laminar flow.

density, the two transport mechanisms act in concert. The reverse is true in the outer region.

Figure 6 presents the profiles of the specific condensation rate given as the sum of the last two terms in equation (15). On a numerical basis, the contribution of the mass nucleation rate $(4/3\pi r^{*3}\rho_l J)$ is negligible in comparison to the growth rate $(\int 4\pi r^2 \dot{r} \rho_l n \, dr)$. The role of the homogeneous nucleation process is relegated to providing condensation sites. This physical picture may be contrasted with ref. [1] in which the direct condensation mechanism was omitted.

### 4.2. *Turbulent flow*

Figure 7 quantifies the influence of boundary layer condensation on $Na_2SO_4$ deposition flux. The results are qualitatively similar to laminar flow except that there is a marked decrease in mass transfer for $T_w \ll T_d$. Also, unlike the laminar flow case, vapor deposition persists even at low surface temperatures. Compared to ref. [1], there is a much faster drop-off in vapor deposition because of the inclusion of direct vapor condensation on entrained particulates.

Figure 8 portrays the turbulent vapor mass fraction profile. Unlike laminar flow, vapor concentration is finite everywhere because of higher turbulent diffusivity.

Figure 9 sketches the aerosol density profile across the particle boundary layer. A non-zero aerosol density extending up to the edge of the boundary layer implies eddy diffusion of the once-nucleated particles into the superheated region where they revaporize.

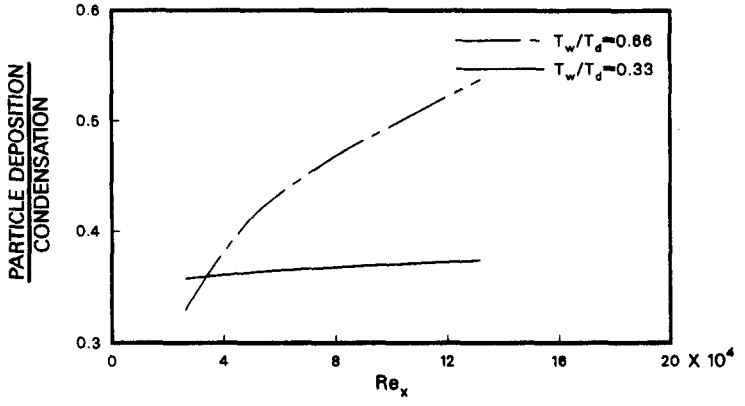


FIG. 2. Particle deposition flux as a fraction of condensation rate in the laminar boundary layer.

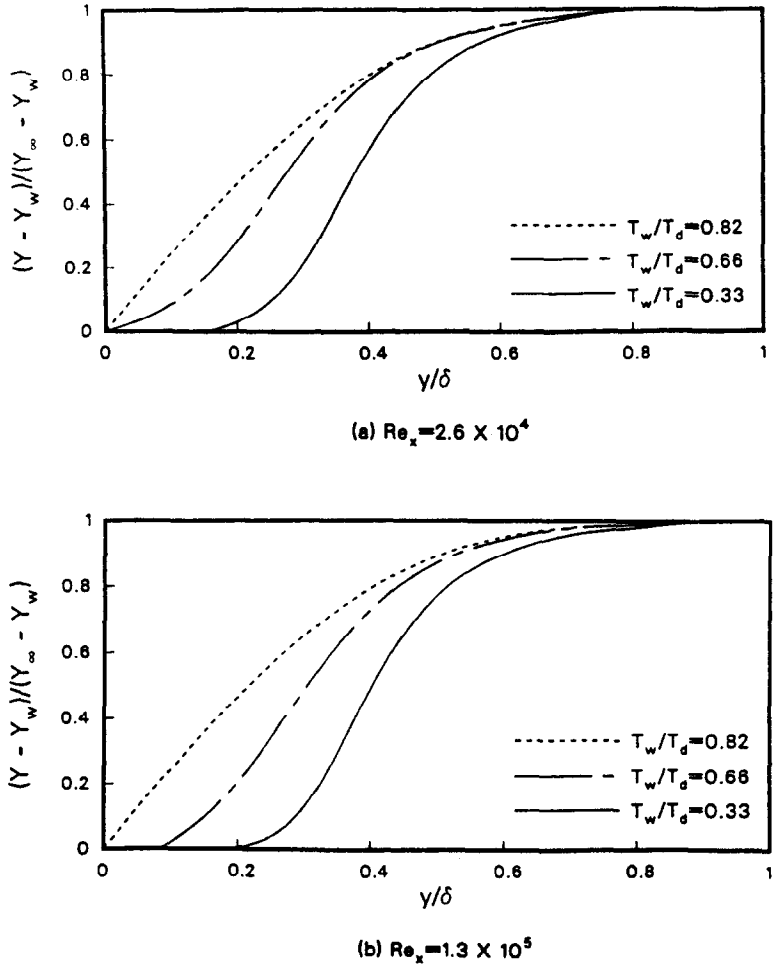


FIG. 3. Effect of boundary layer condensation on laminar vapor mass fraction profile.

This revaporization is, in part, responsible for the significant decline in $Na_2SO_4$ deposition flux because of boundary layer nucleation. At a Reynolds number of $4.2 \times 10^5$ and $T_w/T_d = 0.33$, we calculate that 1% of the condensed mass revaporizes, more than 90% is convected downstream, and only less than 10% is transported to the surface.

Figure 10 shows the transverse variation of the specific condensation rate. As in laminar flow, homogeneous nucleation makes a negligible contribution to

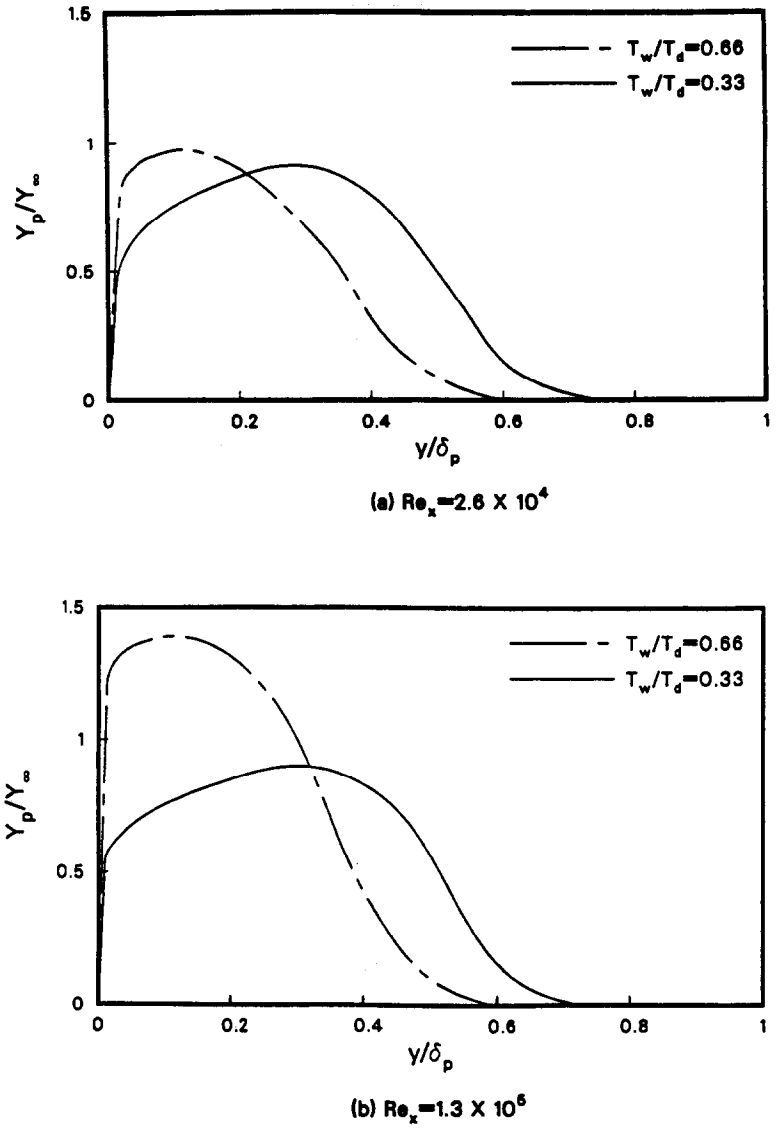


FIG. 4. Aerosol density profile across the laminar boundary layer.

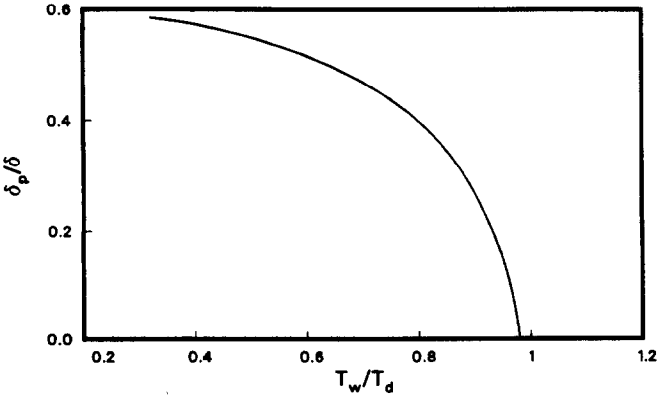


FIG. 5. Laminar particle boundary layer thickness.

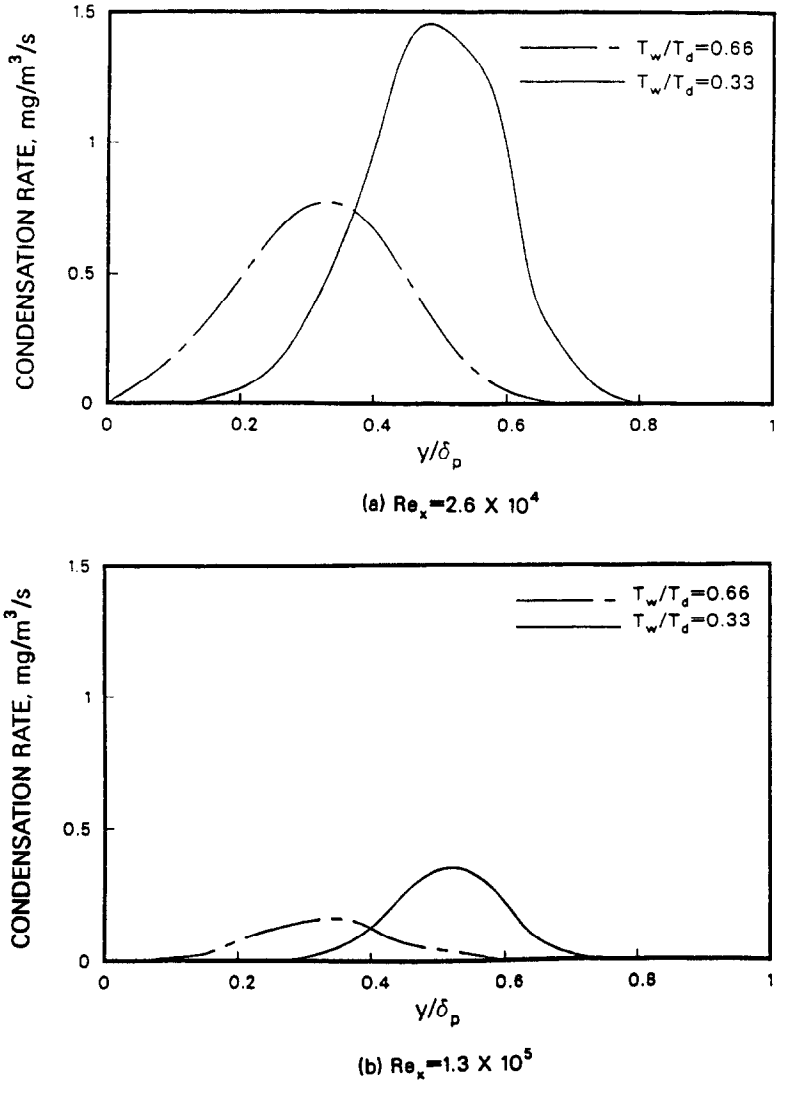


FIG. 6. Vapor condensation rate across the laminar particle boundary layer.

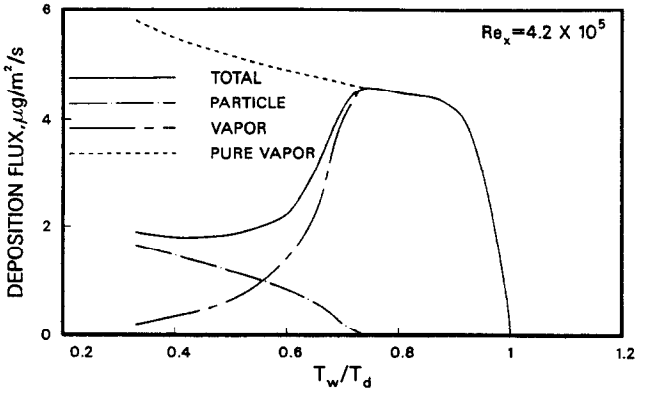


FIG. 7. Particle and vapor deposition in turbulent flow.

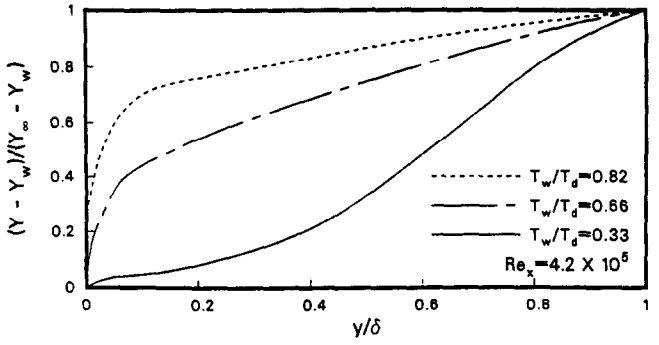


FIG. 8. Turbulent vapor mass fraction profile.

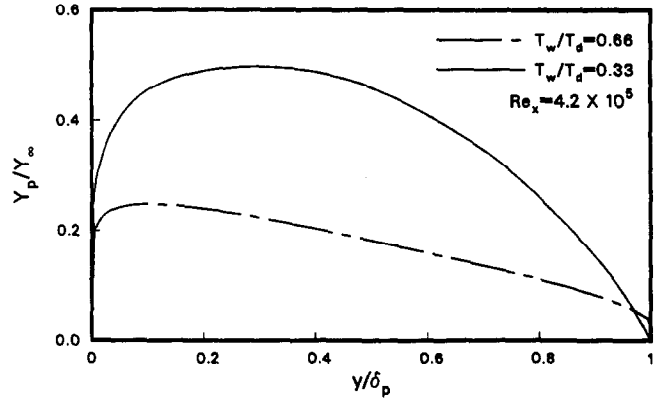


FIG. 9. Aerosol density profile across the turbulent boundary layer.

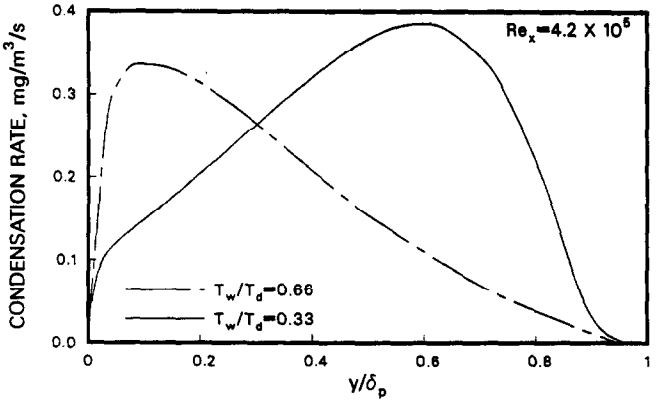


FIG. 10. Specific vapor condensation rate in the turbulent boundary layer.

vapor depletion but is responsible for supplying the condensation sites.

It is useful to represent the combined vapor ($W_v$) and particle ($W_p$) deposition flux in terms of Stanton number for mass transfer ($St_m$) as

$$St_m = \frac{W_v + W_p}{\rho u(Y_\infty - Y_w)}. \quad (21)$$

For a given condensable species, $St_m$ is expected to be a function of Reynolds number ($Re$), Schmidt number ($Sc$), wall subcooling ($T_d - T_w$), free-stream superheat ($T_\infty - T_d$), and pressure

$$St_m = F(Re, Sc, T_d - T_w, T_\infty - T_d, P). \quad (22)$$

Other parameters such as surface tension and latent heat of vaporization that affect nucleation rate should also enter the correlation. Initial attempts to develop the $St_m$ correlation for $Na_2SO_4$ have proved unsuccessful partly because of the complexity introduced by temperature-dependent transport coefficients used

in this study. We intend to conduct a more systematic study of the mass transfer correlation in the future.

On the experimental side, the data of Brown [10] and Santoro *et al.* [11] concerning deposition onto cooled cylindrical targets suggest the existence of boundary layer nucleation phenomena. They too observed a decrease in mass transfer with surface subcooling as predicted by our theory. A direct comparison between theory and experiments has not been possible because of different geometry (flat plate vs cylinder) and other complicating factors such as the possibility of undetermined entrained particulates and deposit runoff in the experimental setup of Santoro *et al.* [11].

## 5. CONCLUSIONS

The problem of boundary layer nucleation has been revisited. A previous model was refined by incorporation of particle convection and heterogeneous nucleation terms in the population balance and vapor conservation equations. It is found that boundary layer nucleation always suppresses the deposition of the impurity vapor. This conclusion overrides the previous result that, for laminar flow, the combined particle plus vapor mass transfer exceeds the value obtained from disregarding the nucleation. Although, in a dust-free gas, homogeneous nucleation is responsible for providing the condensation sites, the actual vapor depletion in the gas phase is found to proceed primarily through the heterogeneous nucleation mechanism.

The decrease in mass transfer due to boundary layer nucleation is more significant in turbulent flow. This is because of the dominating effect of convection such that only a small fraction of condensed mass is transported to the subcooled wall. A similar conclusion was reached in the previous study but for a different reason, namely, turbulent diffusion of the once-nucleated particles across the particle boundary layer into the superheated region.

For both laminar and turbulent flows, an intermediate surface temperature regime is found where impurity mass transfer decreases with subcooling. In this regime, reduction in vapor deposition due to boundary layer condensation is not fully compensated by the ensuing particle deposition.

For laminar flow, a vapor-free zone is formed adjacent to a highly subcooled surface. Its existence is indicative of strong direct vapor condensation on entrained particulates and implies that impurity mass transfer is solely due to particulate deposition mechanisms. For turbulent flow, vapor mass transfer persists at high degrees of subcooling because of higher turbulent diffusivity.

## REFERENCES

1. R. K. Ahluwalia and K. H. Im, Mass transfer of trace species from a superheated stream to a subcooled surface, *Int. J. Heat Mass Transfer* **28,** 2061–2070 (1985).
2. R. K. Ahluwalia and K. H. Im, Vaporization of a heated liquid into a saturated stream, *Int. J. Heat Mass Transfer* **29,** 203–213 (1986).
3. K. H. Im and P. M. Chung, Nucleation and evolution of slag droplets, *A.I.Ch.E. Jl* **28,** 655–663 (1980).
4. K. H. Im, R. K. Ahluwalia and C. F. Chuang, RAFT: a computer model for formation and transport of fission product aerosols in LWR primary systems, *Aerosol Sci. Technol.* **4,** 125–140 (1985).
5. R. K. Ahluwalia and E. D. Doss, Quasi-three-dimensional modeling of flow in MHD channels, *Numer. Heat Transfer* **3,** 67–87 (1980).
6. T. Cebeci and A. M. O. Smith, *Analysis of Turbulent Boundary Layers.* Academic Press, New York (1974).
7. K. H. Im and P. M. Chung, Particulate deposition from turbulent parallel streams, *A.I.Ch.E. Jl* **29,** 498–505 (1983).
8. G. S. Springer, Thermal force on particles in the transition regime, *J. Colloidal Sci.* **34,** 215–220 (1970).
9. N. A. Fuchs, *Evaporation and Droplet Growth in Gaseous Media.* Pergamon Press, London (1959).
10. T. D. Brown, Oil ash deposition, *Fuel* **18,** 28–43 (1967).
11. G. J. Santoro, F. J. Kohl, C. A. Stearns, S. A. Gokoglu and D. E. Rosner, Experimental and theoretical deposition rates from salt-seeded combustion gases of a Mach 0.3 burner rig, NASA TP 2255 (1984).

## NUCLEATION EN COUCHE LIMITE

**Résumé**—On étudie la nucléation et le transport d'une trace condensable d'espèce à travers des couches limites laminaires/turbulentes. La nucléation spontanée homogène se produit pour des surfaces maintenues à des températures beaucoup plus basses que le point de rosée. Les embryons ainsi formés provoquent des sites de condensation pour une nucléation hétérogène. L'effet de la condensation en couche limite est toujours de diminuer le transfert massique des espèces en trace. Il y a un domaine intermédiaire de température où la diminution de dépôt de vapeur n'est pas pleinement compensée par la déposition brownienne thermophorétique des particules, de telle façon que le transfert massique combiné de particules et de vapeur décroît avec le sous-refroidissement de la surface. Pour l'écoulement laminaire, une zone de vapeur libre est adjacente à la surface sous-refroidie par la condensation directe de vapeur sur la matière particulaire entraînée. Le transfert de masse se fait sous l'action des seuls mécanismes de déposition particulaire. Pour l'écoulement turbulent, le transfert massique de vapeur persiste même aux faibles températures de surface. Une décroissance significative dans le flux net de déposition est observée, provenant en partie de la rétrodiffusion turbulente des particules dans la zone surchauffée et, de façon plus importante, de la forte convection turbulente.

## KEIMBILDUNG IN DER GRENZSCHICHT

**Zusammenfassung**—Bildung und Transport eines Kondensationskeims durch unterkühlte laminar/turbulente Grenzschichten werden untersucht. Es zeigt sich, daß die spontane homogene Keimbildung an Oberflächen stattfindet, die auf Temperaturen weit unterhalb des Taupunktes gehalten werden. Die so gebildeten kleinen Tröpfchen verursachen Kondensationspunkte für die heterogene Keimbildung. Der Einfluß der Grenzschichtkondensation ist immer so, daß er den Massentransport der Keimlinge vermindert. Es gibt einen mittleren Temperaturbereich, in dem die Abnahme der Dampfabscheidung nicht vollständig durch die folgende Brown'sche/thermophoretische Abscheidung von Makroteilchen kompensiert wird, so daß der kombinierte Teilchen- und Dampfmassentransport mit der Wandunterkühlung abnimmt. Bei laminarer Strömung entsteht eine dampffreie Zone in der Nähe der unterkühlten Oberfläche durch direkte Dampfkondensation an den mitgerissenen Teilchen. Der Massentransport erfolgt allein aufgrund von Abscheidungsmechanismen an Makroteilchen. Bei turbulenter Strömung hält der Dampfmassentransport nur bei geringen Oberflächentemperaturen an. Eine signifikante Abnahme in der Nettodampfrate wird beobachtet, teilweise aufgrund von turbulenter Rückdiffusion von Teilchen in die überhitzte Zone und insbesondere durch starke turbulente Konvektion.

## НУКЛЕАЦИЯ В ПОГРАНИЧНОМ СЛОЕ

**Аннотация**—Исследуется образование зародышей новой фазы и перенос ряда конденсирующихся индикаторных веществ через переохлажденные ламинарные турбулентные пограничные слои. Найдено, что спонтанное однородное образование зародышей происходит при таких условиях, когда значение температуры поверхности поддерживается намного ниже точки росы. Образованные таким образом зародыши служат центрами для гетерогенной нуклеации. Во всех случаях конденсация в пограничном слое снижает массоперенос индикаторных веществ. В некотором промежуточном диапазоне тмператур конденсация пара не полностью компенсируется последующим броуновским или термофорезным осаждением макрочастиц, вследствие чего смещанный массоперенос частиц и пара уменьшается с уменьшением переохлаждения поверхности. В случае ламинарного течения из-за прямой конденсации пара на переносимых частицах вещества образуется свободная от пара зона, прилегающая к недогретой поверхности. Тогда массоперенос осуществляется только путем осаждения частиц. При турбулентном течении массоперенос пара происходит даже при низких температурах поверхности. Значительное уменьшение суммарного потока осаждающегося вещества происходит частично вследствие турбулентной диффузии в перегретую зону и, в большей степени, вследствие сильной турбулентной конвекции.